European Polymer Journal 209 (2024) 112910

Contents lists available at ScienceDirect

European Polymer Journal

journal homepage: www.elsevier.com/locate/europolj

Improved electro-destruction of bacterial biofilms by coating conductive surfaces with polymers

Stephane Hoang [a,b], Hanna Zhukouskaya [a], Iryna Ivanko [a], Jan Svoboda [a], Michaela Hympánová [c], Jan Marek [c,d,*], Ondřej Soukup [c], Miroslav Šlouf [a], Jan Kotek [e], Eric Doris [b], Edmond Gravel [b], Elena Tomšík [a,*], Martin Hrubý [a,*]

[a] Institute of Macromolecular Chemistry CAS, Heyrovského náměstí 2 162 06, Prague 6, Czech Republic
[b] Université Paris-Saclay, CEA, INRAE, Département Médicaments et Technologies pour la Santé (DMTS), SCBM, 91191, Gif-sur-Yvette, France
[c] Biomedical Research Centre, University Hospital Hradec Králové, Sokolská 581 500 05, Hradec Králové, Czech Republic
[d] Department of Epidemiology, Military Faculty of Medicine, University of Defence in Brno, Třebešská 1575, 500 05, Hradec Králové, Czech Republic
[e] Department of Inorganic Chemistry, Faculty of Science, Charles University, Hlavova 8 12840, Prague 2, Czech Republic

ARTICLE INFO

Keywords:
Bacteria
Biofilm
Polymer
Anodic oxidation
Ferrocene
Staphylococcus aureus

ABSTRACT

The formation of biofilm involves cell aggregation and adherence, enveloped by a self-produced extracellular matrix. In the medical domain, biofilm-associated infections pose significant challenges, especially concerning implants. This investigation focuses on enhancing electromediated bacterial biofilm eradication through polymer coatings on the anode. These coatings catalyze reactive oxygen species (ROS) generation or convert hydrophobic coatings to bactericidal hydrophilic polycations, detaching the biofilms that are predominantly polyanionic. The first approach employs a metallized polytetrathienylporphyrin layer with ROS catalytic capability, while the second involves an insoluble hydrophobic polyamide, which, upon oxidation, transforms into a bactericidal hydrolytically degradable polycation. Both approaches show promising efficacy in augmenting electromediated *Staphylococcus aureus* biofilm destruction.

1. Introduction

Bacteria, and at times fungi as well, exhibit a remarkable adaptive response in the face of hostile environments. This response entails the formation of a complex biofilm structure, wherein cells aggregate and adhere both to one another and to the solid substrate. This aggregate is embedded in the extracellular matrix which cells form through collective quorum-sensing communication.[1] This intricate process unfolds through several distinct stages: an initial attachment phase, followed by the assembly of microcolonies, the progression into a nascent biofilm, the maturation into a highly organized biofilm structure, and ultimately, the dispersion that occurs under stressful conditions.[2,3] The initiation of adhesion is caused by the secretion of extracellular polymeric substances. These substances, containing a mixture of polysaccharides, extracellular DNA, proteins, lipids and amyloid fibrils, play a crucial role in initiating and stabilizing the adhesion process. As microcolonies take shape, they begin to form a protective hydrogel layer. In the mature biofilm stage, a stratified arrangement emerges, featuring layers of macrocolonies interconnected by channels that facilitate the distribution of nutrients and signaling molecules.[3] The significance of such a complex architecture becomes evident in the face of antimicrobial challenges. Biofilms exhibit a range of antibiotic resistance mechanisms. These mechanisms include a suppressed metabolism, the persistence of dormant cells,[4] and the emergence of highly resilient variant colonies.[1,5,6].

Under stress, biofilms trigger specific responses that can lead to a range of consequences. These include hindrance of drug penetration, alterations in the chemical microenvironment, and an increase in the expression of genes responsible for drug resistance. Consequently, the eradication of bacterial biofilms proves to be a formidable challenge, as they effectively shield the resident bacteria from both antibiotic treatments and immune response.[1,4,5].

In the realm of medicine, the formation of pathogenic bacterial biofilms presents a particularly vexing issue, especially in association with medical implants such as catheters, prosthetic joints, stents, and trauma hardware.[6–9].

* Corresponding authors.
E-mail addresses: jan.marek@fnhk.cz (J. Marek), tomsik@imc.cas.cz (E. Tomšík), mhruby@centrum.cz (M. Hrubý).

https://doi.org/10.1016/j.eurpolymj.2024.112910
Received 20 November 2023; Received in revised form 5 March 2024; Accepted 7 March 2024
Available online 8 March 2024

Currently, chemical approaches encompass several options for curbing biofilm formation or undermining its stability.[1,5,6,10,11] First, non-biofouling surfaces are employed, designed to hinder the adhesion of bacterial cells and the extracellular matrix.[6,10] While these surfaces offer some prevention, their long-term efficacy is often limited. In fact, once a biofilm establishes itself on a part of the surface, it serves as a platform for further expansion.

Second, there are cationic surfaces with inherent bactericidal properties.[11,12] However, these surfaces tend to exhibit toxicity towards not only bacterial cells but also eukaryotic cells, and they can adsorb blood plasma proteins.

Third, there are strategies involving the controlled release of bactericidal or bacteriostatic agents, such antibiotics or as silver ions sourced from silver nanoparticles.[5,13] While this approach is exploitable, it carries the risk of fostering the development of resistant bacterial strains.

Alternatively, a fourth avenue entails the use of nucleases, enzymes capable of cleaving DNA, which is a pivotal constituent maintaining biofilm integrity.[11,14,15] DNase, a nuclease, has proven to be highly effective, particularly in the initial 12-hour window.[15] However, its effectivity diminishes thereafter due to degradation by proteases. Another strategy involves quorum-sensing inhibitors that limit bacteria coordination and cooperation.[5].

While each approach offers certain advantages, they also come with inherent limitations that reduce the effectivity of the method. Thus, the complexity of biofilm management necessitates a careful consideration of the various strategies available.

While a multitude of pharmaceutical strategies are aimed at combatting drug resistance in biofilms, there exists a realm of physical energy-based methodologies that present viable alternatives.[2,6,8,9] These approaches include not only the direct annihilation of biofilms but also the augmentation of pharmaceutical agent efficacy. Predominantly, these techniques encompass photodynamic biocidal treatment facilitated by, *e.g.*, photogenerated singlet oxygen,[8] the application of biocidal radiation,[16] plasma treatment,[17] or the application of electric current.[7,9].

The utilization of electric current has been under investigation due to its influence over both prokaryotic and eukaryotic cells.[2,7,18] These effects are hypothesized to emanate from processes such as electrolysis, the oxidation of enzymes and coenzymes and the impairment of cellular membranes.[2,7,9,18].

The observed electricidal effect associated with direct current (DC) has been attributed to the generation of reactive oxygen species (ROS), rather than biofilm detachment.[2,18,19] The combination of DC with ROS-scavenging antioxidants, such as catalase, mannitol, and tempol, yields a marked reduction in bactericidal effects of DC, showing the importance of electrogenerated ROS in the process.[19] The use of DC, either alone or in combination with antibiotics, promises innovative ways to treat biofilms. Furthermore, the efficacy of electricidal effects against a range of Gram-positive and Gram-negative species has been convincingly demonstrated.[2].

There are questions about the effectiveness and the optimal choice of electric current – whether direct current or alternating current – for facilitating biofilm detachment. Preliminary investigations have underscored the potential of DC in augmenting the potency of tobramycin, resulting in a substantial diminishment of *Pseudomonas* biofilm.[20] This phenomenon, known as the "bioelectric effect",[18] arises when low-intensity direct current electric fields are combined with biocides and antibiotics.

In this investigation, we focused on augmenting the electromediated eradication of bacterial biofilms through the application of polymer coatings on the anode. These coatings possess dual functions: i) the catalytic promotion of bactericidal ROS formation through electrolysis on the electrode surface, and ii) the use of the ROS generated *via* electrolysis to convert initially electroneutral hydrophobic polymer coatings into bactericidal hydrophilic polycations, which desorb from the anode together with bound polyanionic biofilms (see Fig. 1 for an illustrative diagram). The real-life application would be as a polymer coating of electrically conductive or semiconductive surfaces that can be on-demand sterilized by applying low (ca 2 V) voltage for a short time. Making the necessary voltage as low as possible and electric treatment as short as possible is highly desirable for potential bio-related applications.

The first approach, *i.e.* the catalytic approach, leverages a metallized layer of polytetrathienylporphyrin. This chemistry, previously developed for ROS detection,[21] has been exceptionally successful in ROS generation when a potentiometric setup is changed to an electrolytic configuration. The first strategy is therefore based on ROS generation by polymer layer-catalyzed electrooxidation of water.

The second method, referred to as cation generation, centers on an insoluble, hydrophobic polyamide derived from 1,6-diaminohexane and 1,1′-ferrocenedicarboxylic acid. The ferrocene moiety in its iron(II) state displays hydrophobicity, a lack of charge, orange hue, diamagnetism, and hydrolytic stability. Upon oxidation, the ferrocene moiety transforms into ferrocenium(+) with iron(III), resulting in a hydrophilic, cationic, blue-green species that is paramagnetic, water-soluble and hydrolytically labile. Given the presence of multiple ferrocene moieties in one chain, as is the case here, the outcome is the formation of a potentially bactericidal hydrolytically degradable polycation (see Scheme S1 for suggested structures).

Both of these novel approaches have demonstrated remarkable enhancement of the electromediated destruction of *Staphylococcus aureus* biofilms.

2. Materials and methods

2.1. Materials

The following materials were used: graphite rods (KOH-I-NOOR HARDTMUTH a.s. Czech Republic), 3,3,5,5-tetramethylbenzidine (Sigma-Aldrich Ltd., Prague, Czech Republic), chloroform stabilized with amylene (pure, Sigma-Aldrich Ltd., Prague, Czech Republic), formic acid (98 %, Sigma-Aldrich Ltd., Prague, Czech Republic), manganese(II) chloride monohydrate (>97 %, Sigma-Aldrich Ltd., Prague, Czech Republic), iron(II) chloride (>99 %, Sigma-Aldrich Ltd., Prague, Czech Republic), *N,N*-dimethylacetamide (Sigma-Aldrich Ltd., Prague, Czech Republic), 1-methylimidazole (97 %, Sigma-Aldrich Ltd., Prague, Czech Republic), succinic acid (Sigma-Aldrich Ltd., Prague, Czech Republic). All other chemicals were purchased from Lach-Ner Ltd. (Neratovice, Czech Republic). All aqueous solutions were prepared from deionized water (DIW).

2.2. Instruments

Electrochemical deposition of 5,10,15,20-tetra(thien-3-yl)porphyrin (3TTP) was performed using an AUTOLAB PGSTAT302N potentiostat with FRA32M Module and Nova software 2.1. Electrochemical deposition was carried out using three-electrode set up: Pt electrode with an area of 1.2 cm^2 served as a counter electrode and Ag/AgCl was utilized as a pseudo-reference electrode.

The X-ray photoelectron spectroscopy (XPS) measurements were performed using a K-Alpha + XPS spectrometer (ThermoFisher Scientific, UK) operating at a base pressure of $1.0 \bullet 10^{-7}$ Pa. The data acquisition and processing were performed using the Thermo Avantage software. All samples were analyzed using a microfocused, monochromated Al Kα X-ray radiation (400 μm spot size) with pass energy of 200 eV for survey and 50 eV for high-energy resolution core level spectra. The X-ray angle of incidence was 30° and the emission angle was along the surface normal. The binding energy scale of the XPS spectrometer was calibrated by the well-known positions of the C 1 s C–C and C–H, C–O and C(=O)–O peaks of polyethylene terephthalate and Cu 2p, Ag 3d, and Au 4f peaks, respectively. The obtained high-

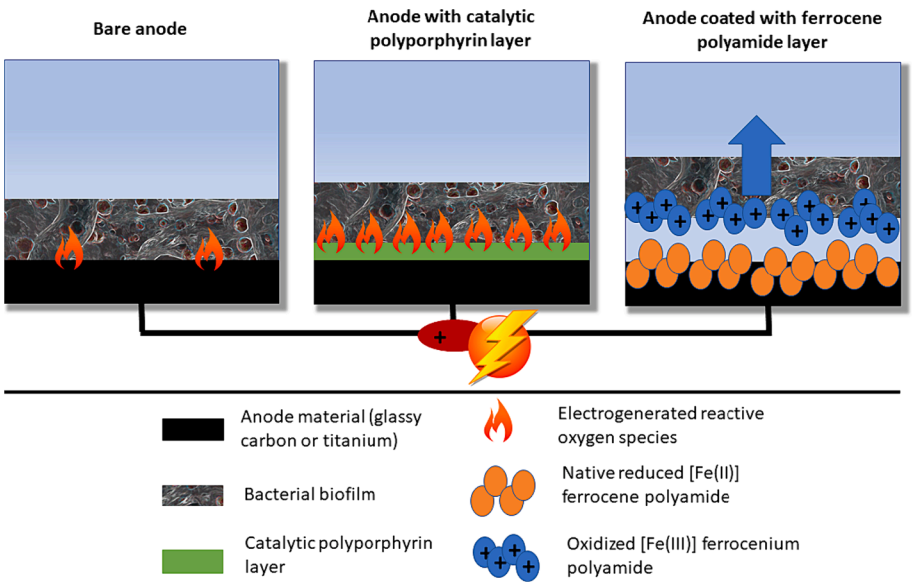

Fig. 1. Approaches used in this study to enhance destruction of bacterial biofilm by electrolysis using surface-coated anode with designed polymers.

resolution spectra were fitted with Voigt profiles to probe the individual contributions of present chemical species.

The absorption spectra of 3TTP/Me in the chromogenic solution was performed using an AvaSpec-ULS2048L spectrophotometer (Avantes).

Scanning electron microscopy (SEM) of poly-3TTP/Fe films was performed with a high-resolution SEM microscope MAIA3 (TESCAN, Czech Republic). The samples for SEM were sputtered with a thin platinum layer (thickness ~ 5 nm) using a vacuum sputter coater SCD 050 (Leica, Austria), in order to minimize possible electron beam damage and charging. The observations were made in high vacuum at accelerating voltage of 3 kV using secondary electron (SE) detector.

2.3. Electrodeposition of polytetrathienylporhyrin (poly-3TTP) layer on electrode surface

The 5,10,15,20-tetra(thien-3-yl)porphyrin (3TTP) was synthesized according to the recently published procedure.[21] The graphite rods with the length of 2 cm were used as an electrode substrate for the anode based on the polyporphyrin / polyamide layers. Prior to the electropolymerization of 3TTP, the electrode substrate used as a working electrode (WE) was rinsed thoroughly with ethanol and acetone for 10 min by ultrasonication. The electro-polymerization of 1.3 mM (12 mg) 5,10,15,20-tetra(thien-3-yl)porphyrin (3TTP) dissolved in 7.5 M formic acid and 0.25 mM 1-methylimidazole in CH_2Cl_2 (10 mL) was performed in a three-electrode cell (total volume 15 mL) with an AUTOLAB PGSTAT302N potentiostat. We controlled the distance between the working, reference and counter electrodes with the holder where fixed position for the three electrodes are made. Moreover, the working electrodes had the same size and were immersed into the polymerization solution to the identical depth. All measurements were carried on at an ambient temperature by cycling the potential 30 times between − 1.00 and 1.85 V with a scan rate of 50 mV s^{-1}. The polymerization solution was purged with N_2 gas for 15 min prior to each electro-polymerization. The solution was blanketed with N_2 during electro-polymerization to protect it from atmospheric oxygen.

2.4. Preparation of metal-complexed poly-3TTP (3-TTP/Me)

Metal cations Fe^{2+} or Mn^{2+} were incorporated into the porphyrin core by the dipping of individual poly-3TTP electrodes into the 0.1 M aqueous solutions of the corresponding metal chloride for 24 h. To prove the chelating of corresponding metals into the porphyrin core the XPS spectra were recorded.

2.5. Synthesis of ferrocene polyamide (Fc-PA)

To a suspension of 1,1′-ferrocenedicarboxylic acid (1.0 equiv., 0.73 mmol, 200 mg) in anhydrous chloroform (4 mL) was added anhydrous *N,N*-dimethylformamide (200 μL). Then oxalyl chloride (4.0 equiv., 2.9 mmol, 245 μL) was added dropwise under vigorous stirring and argon atmosphere. The reaction mixture was stirred for 5 h at room temperature. During the addition of oxalyl chloride, the mixture turned from an orange suspension to a clear red homogeneous solution, showing the transformation of the diacid to the corresponding di-acyl chloride. Excess of oxalyl chloride and solvent were evaporated under vacuum to afford 224 mg of the desired 1,1′-ferrocenedicarboxylic acid dichloride ($Fc(COCl)_2$) as a red solid. The resulting product was used without further purification to avoid hydrolysis.

A solution of $Fc(COCl)_2$ (1.0 equiv., 0.73 mmol, 224 mg) in chloroform (5 mL) was added to an aqueous solution (5 mL) of sodium carbonate (4.0 equiv., 2.9 mmol, 305 mg) and 1,6-hexanediamine (0.9 equiv., 0.64 mmol, 74 mg). The addition led to a rapid formation of a solid at the solvents interface. After 20 min of standing at room temperature, the heterogeneous mixture was stirred vigorously for 15 h. The visible brown precipitate was recovered by centrifugation at 7830 rpm for 15 min. Then, the solid was suspended in water and filtered. Several washes with water and then with acetone were performed to remove by-products. The resulting solid was dried in the oven at 100 °C for 1 h to afford a brown solid (56 mg) that is only soluble in very acidic media such as pure formic acid.

^{1}H NMR (400 MHz, d-formic acid) δ (ppm): 4.82 (Cp, 4H), 4.56 (Cp, 4H), 3.24 (4H, –CH_2–NHCO), 1.50–1.27 (8H, –CH_2–). ^{13}C NMR (100 MHz, $CDCl_3$) δ(ppm): 172 (–NHCO–), 76–68 (Cp), 40 (–CH_2–NH), 27–25 (–CH_2–). FTIR (cm^{-1}): 3261 (N–H), 2933 (C–H), 1624 (C = O).

2.6. Coating of electrodes with Fc-PA

The electrode was fully immersed in an ethanol solution and sonicated for 10 min. The procedure was repeated once more with acetone. Once dry, the electrode was partly dipped into a solution of Fc-PA (5 mg) in formic acid (1 mL) for 10 sec. The electrode was then dried under vacuum overnight to evaporate formic acid. The resulting electrode was then used for the antibacterial tests.

2.7. Electro-formation of ROS in vitro

The chromogenic agent 3,3,5,5-tetramethylbenzidine was used to prove the formation of ROS during the direct evolution of oxygen on the anode consisting of poly-3TTP/Me. The powdered 3,3,5,5-tetramethylbenzidine (to the final concentration of 2.7 mM) was dissolved in 0.1 M succinic acid and 7.7 M *N,N*-dimethylacetamide in water (pH of solution was 4.7). The spectro-electrochemical measurements were performed in quartz cuvette in three-electrode cell configuration: Pt wire as counter electrode, Ag/AgCl as a pseudo-reference electrode. Potentials in the range of 1.1–2.0 V *vs.* Ag/AgCl were applied to poly-3TTP/Me for 10 s.

2.8. Electro-degradation of poly-3TTP/Me or ferrocene polyamide surfaces

The test of electrochemical stability of poly-3TTP/Me or ferrocene polyamide surfaces were performed under chrono-potentiometric measurement: the constant 2 V was applied during 10 min at working electrodes. The measurements were repeated 3 times. The surface of the electrodes before and after applying constant potential was studied by scanning electron microscopy measurements.

2.9. Testing antibacterial activity: Biofilm formation and antimicrobial activity evaluation

Staphylococcus aureus ATCC 25923 was obtained from Czech Collection of Microorganisms. Prior to experiments, 2–3 colonies from fresh secondary culture were suspended in Trypticase soya broth (TBS; HiMedia, Cadersky-Envitek, Prague, Czech Republic) and grown for 8 h under aerobic conditions at 37 °C, 120 rpm to achieve bacterial culture at exponential growth phase. Subsequently, the culture was diluted 1:100 in Brain heart infusion broth (BHI; HiMedia, Cadersky-Envitek, Prague, Czech Republic) and 500 μL of final inoculum was transferred into well of sterile deep 96-well plate. Previously disinfected (30 min immersion in 70 % ethanol) electrodes were then individually placed into wells containing bacterial inoculum. The biofilm was formed for 24 h at 37 °C and 180 rpm.

Biofilms grown on electrodes were rinsed with 0.9 % NaCl solution to remove unattached bacteria and immersed in 0.9 % NaCl solution with or without Catalase 300–750 UI/mL (Catalase from bovine liver, Merck Life Science spol. s r.o., Czech Republic). Then, the coated electrodes were connected as anodes to electrical circuit and biofilms were exposed to electric current for 20 min at constant voltage of 2.0 V. After exposure, the electrodes were transferred to tubes containing 1 mL of BHI and sonicated for 5 min to disrupt remaining biofilm and release bacteria into broth. Remaining bacteria were quantified by plate counting assay.

Mann-Whitney test was used to analyze obtained results, where P-values of < 0.05 were considered to be significant. All statistical analyses and corresponding graphical representation were performed by GraphPad Prism 6.04 software (GraphPad Software Inc., San Diego, California, USA).

2.10. Antimicrobial activity of the oxidized Fc-PA in solution

Previously disinfected Fc-PA coated electrodes were immersed in 0.9 % NaCl solution and connected as anodes to electrical circuit for 20 min at a constant voltage of 2.0 V (similar condition as biofilm treatment) to obtain 0.9 % NaCl solution containing oxidized Fc-PA. Then 900 μL of the solution was mixed with 100 μL of *S. aureus* ATCC 25923 suspension (approximately 108 CFU/ml in 0.9 % NaCl). The influence of solution containing oxidized polyferrocene on bacteria was determined after 20 min exposure time by plate counting assay.

3. Results and discussion

The initial method concerned the electrochemical generation of reactive oxygen species at the surface of the anode. Notably, recent research conducted by our team demonstrated the electrochemical synthesis and deposition of poly-3TTP onto carbon rods (CR).[21] In the present investigation, we extended this approach by depositing poly-3TTP films onto CR, subsequently complexing metal ions such as Mn^{2+} and Fe^{2+} within the porphyrin rings. This process aimed to finely adjust the catalytic electrochemical attributes of the ROS-generating stratum. The inclusion of metal ions within the poly-3TTP layers was unequivocally verified via high-resolution core-level X-ray Photoelectron Spectroscopy (XPS) analysis. Detailed results can be found in Fig. 2, which illustrates the scenarios for Mn^{2+}- and Fe^{2+}-doped poly-3TTP, in contrast to the original non-metallized poly-3TTP layers.

Deconvolution of the high-resolution core-level XPS spectrum focused on the N 1 s level of poly-3TTP unveils two distinct peaks. These peaks correspond to oxidized pyrrole units (=N–, at 400 eV) and reduced pyrrole units (–NH–, at 401 eV) within the porphyrin structure (see Fig. 2). Upon integration of metal ions into the system, the XPS spectrum undergoes notable changes. A new peak emerges, accompanied by a significant reduction in the intensities of the peaks associated with the metal-free porphyrin structure. The new additional peaks correspond to nitrogen atoms forming complexes with the respective metal ions.

The emergence of ROS under a consistently applied potential was affirmed by assessing UV–Vis spectra while 3,3,5,5-tetramethylbenzidine was present. It is widely acknowledged that during anodic oxidation, water molecules have the propensity to yield hydrogen peroxide by the chemical reactions shown below:

$$O_2 + 4H^+ + 4e^- \rightarrow 2H_2O \; E_0 = +1.23 \text{ V}$$

$$2O_2 + 4H^+ + 4e^- \rightarrow 2H_2O_2 \; E_0 = +0.70 \text{ V}$$

$$2H_2O + O_2 \rightarrow 2H_2O_2 \; \Delta E = -0.53 \text{ V}$$

Detection of ROS formation was accomplished by monitoring the alteration in color of the chromogenic agent (Fig. 3). All spectro-electrochemical measurements were conducted in a light-restricted environment within the Faraday cage to shield against electromagnetic interference.

Previous study[22] has documented the oxidation of 3,3,5,5-tetramethylbenzidine (TMB) by H_2O_2. This oxidation process yields either bi-cation radical or a fully oxidized product, as illustrated in Fig. 3a. Notably, the absorption peak for the initial stage of oxidation resides at 652 nm, while the fully oxidized state exhibits a peak at 452 nm. The spectral evolution of poly-3TTP/Mn and poly-3TTP/Fe is depicted in Fig. 3b and 3c, respectively, contingent upon the applied oxidation potential. Both polymer complexes affirm that, upon maintaining a constant potential, H_2O_2 forms and interacts with TMB molecules. Intriguingly, it is observed that, in the case of poly-3TTP/Mn, the full oxidation state is only registered following the application of a 2 V potential (Fig. 3b). In contrast, a fully oxidized state was formed for poly-3TTP/Fe at an applied potential as low as 1.1 V and the consequent potential increase to 2 V had no visual effect (Fig. 3c).

Based on these findings, we deduce that poly-3TTP/Fe demonstrates a greater propensity to catalyze the formation of H_2O_2 compared to poly-3TTP/Mn. As metal ion matters, the ROS generation is most plausibly catalysed by the polytetrathienylporphyrine-complexed metal ion so the exact ROS-generation mechanism may vary depending on the metal ion type. Consequently, poly-3TTP/Fe was chosen for further antibacterial activity assessments. Furthermore, from the absorption spectroscopy data, a constant potential of 2 V was deemed suitable for subsequent measurements.

The second approach, referred to as cation generation, focuses on an insoluble and hydrophobic ferrocene polyamide (Fc-PA) coating synthesized from 1,6-diaminohexane and 1,1′-ferrocenedicarboxylic acid.

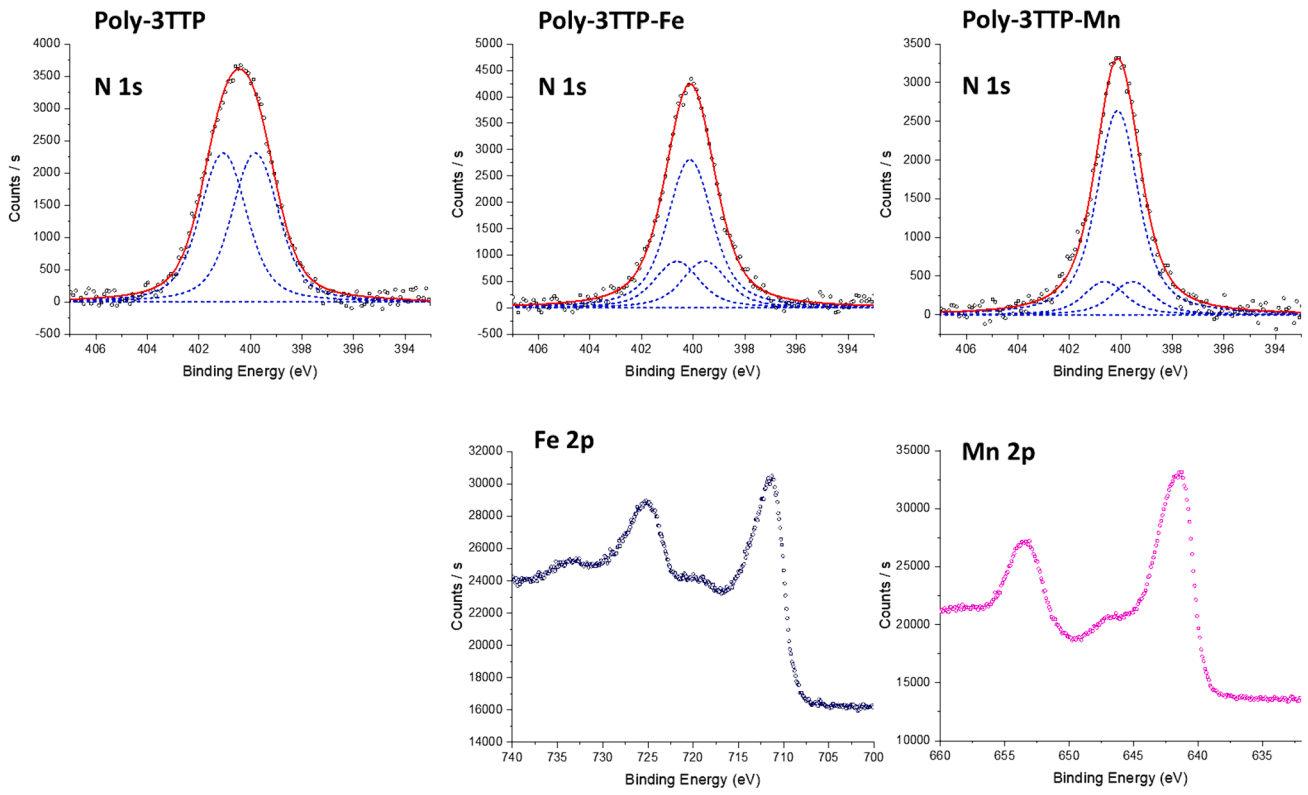

Fig. 2. The high-resolution XPS spectra of polyporphyrin with Mn^{2+} and Fe^{2+} ions: upper row) N 1 s spectra of poly-3TTP, poly-3TTP/Fe and poly-3TTP/Mn; lower row) Mn 2p and Fe 2p spectra of corresponding ions. The XPS spectrum of pure poly-3TTP is presented for comparison.

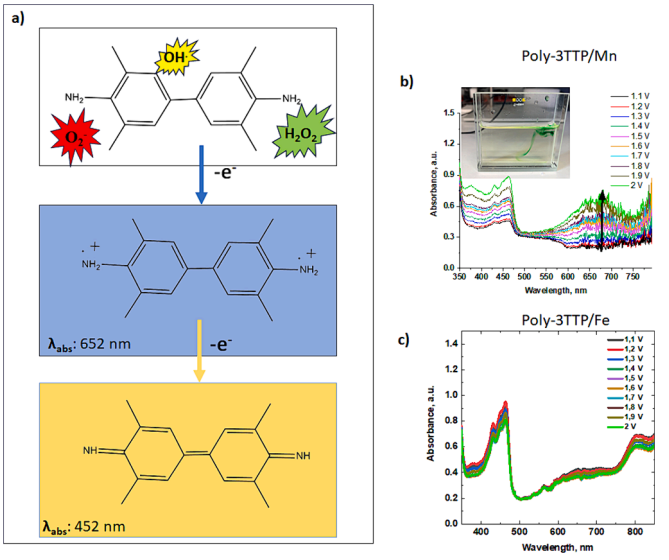

Fig. 3. a) depiction of the chemical structure of 3,3,5,5-tetramethylbenzidine across various redox states; b) uv–Vis spectra portraying the electrochemically generated dye on the poly-3TTP/Mn anode layer at distinct applied potentials (Insert: visual appearance); c) UV–Vis spectra illustrating the electrochemically generated dye on the poly-3TTP/Fe anode layer across varying applied potentials.

The ferrocene moiety, in its iron(II) state, exhibits traits such as hydrophobicity, neutrality in charge, orange color, diamagnetism, and resistance to hydrolysis. Upon oxidation, the ferrocene moiety transforms into ferrocenium(+) with iron(III), leading to the formation of a hydrophilic, cationic, blue-green species that is paramagnetic, water-soluble, and prone to hydrolytic degradation.[23,24] Given the presence of multiple ferrocene moieties within the same chain, as demonstrated here, the outcome is the development of a potentially antibacterial hydrolytically degradable polycation. The Fc-PA was synthesized through classical interphase polymerization using 1,1′-ferrocenedicarboxylic acid chloride in an organic solvent and 1,6-diaminohexane in an aqueous phase with sodium carbonate as a by-product-removing base. The resulting product's structure was verified using NMR spectroscopy. The glassy carbon (GC) electrode was coated with this polyamide by dip-coating it from a solution in formic acid.

To confirm that poly-3TTP/Fe films maintain their structural integrity while the ferrocene polyamide films undergo polymer ablation following the application of a constant current, scanning electron microscopy was employed to analyze the surface of the polymer films before and after chrono-potentiometry. The outcomes of these investigations are outlined in Fig. 4a and 4b for poly-3TTP/Fe, and Fig. 4c and 4d for the ferrocene polyamide. Remarkably, there is no significant alteration observed in the catalytically active poly-3TTP/Fe film, substantiating its durability. In contrast, as anticipated, noticeable polymer ablation is evident in the ferrocene polyamide layer, which is inherently sensitive to electrooxidation. The large-scale bar images are presented in SI Figure S1 for poly-3TTP/Fe and Figure S2 for Fe-PA.

3.1. Antimicrobial activity evaluation

The population of bacteria within the biofilm developed on Fc-PA and Poly-3TTP/Fe-coated electrodes demonstrated a notable reduction subsequent to exposure to a 2 V potential for 20 min (see Fig. 5). The logarithmic reduction (log R) values, defined as logarithm of the proportion of surviving bacteria without application and with application of voltage, was 3.8 for Fc-PA and 4.7 for Poly-3TTP/Fe. While a decline in bacterial numbers was also observed on non-coated electrodes, the reduction was significantly lower (log $R = 2.7$). We also tested whether the released oxidized FC-PA release would eventually cause antibacterial activity in solution. Obviously in our case the lifetime of the oxidized

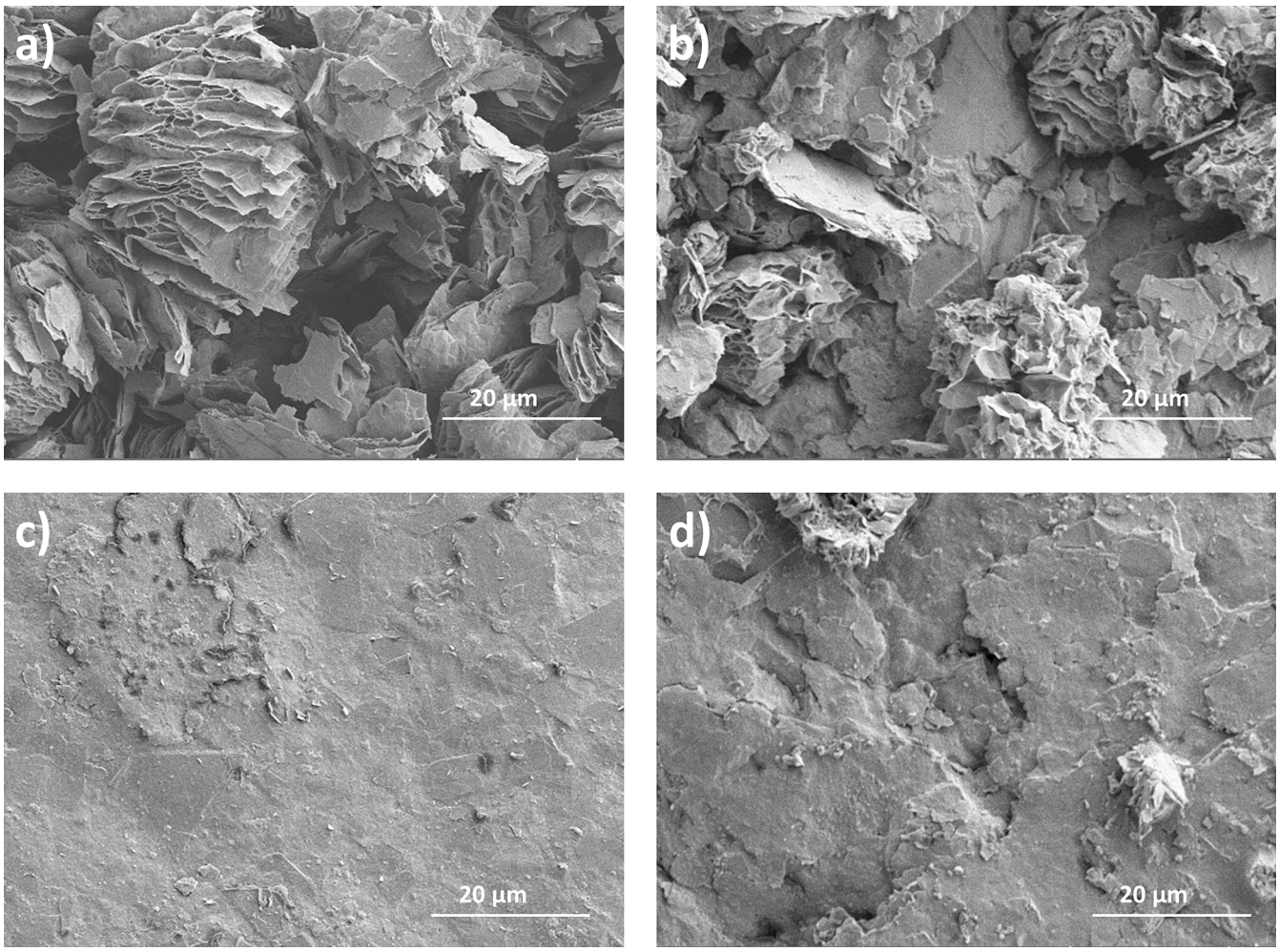

Fig. 4. SEM micrographs of a) poly-3TTP/Fe original film surface, b) poly-3TTP/Fe after chrono-potentiometric measurement, c) Fc-PA original film surface and d) Fc-PA film surface after chrono-potentiometric measurements.

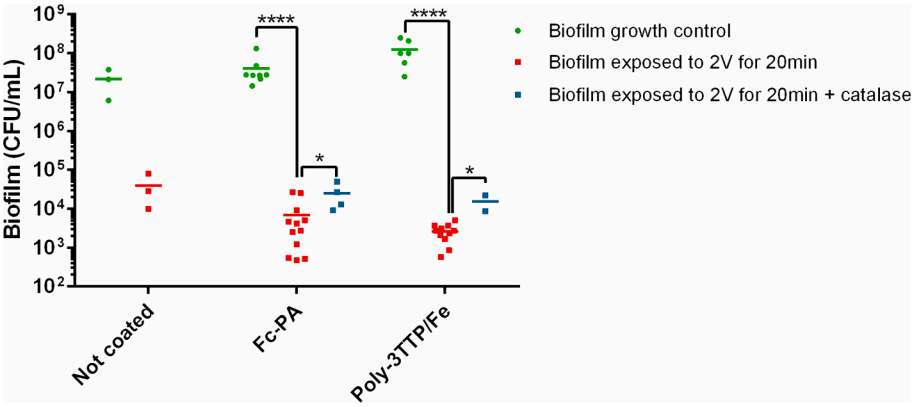

Fig. 5. Survival of bacteria *Staphylococcus aureus* in biofilms cultivated on uncoated electrodes, electrodes coated with ferrocene polyamide (Fc-PA), and Poly-3TTP/Fe-coated electrodes. The results highlighted in green denote untreated biofilms. The results presented in red pertain to biofilms subjected to a 2 V potential for 20 min. Biofilms exposed to a 2 V potential for 20 min in the presence of 300–750 UI/mL catalase are represented in blue. Individual values from each measurement are depicted as data points, while group averages are indicated by lines. Statistical significance: * ($p < 0.05$); **** ($p < 0.0001$). (For interpretation of the references to color in this figure legend, the reader is referred to the web version of this article.)

ferrocenium (oxidized) polymer against hydrolysis is rather short, so the antibacterial effect remains local in close proximity of the layer not contaminating the whole volume of the solution with potentially cytotoxic cation, no antibacterial activity was found in solution after hydrolysis.

The discernible antimicrobial impact stemming from ROS release is corroborated by a significant contrast in bacterial reduction under conditions with and without catalase (log *R* equal to 3.2 and 3.9 in the presence of catalase for Fc-PA and Poly-3TTP/Fe, respectively). This substantiates that the generation of hydrogen peroxide through anodic

oxidation holds a pivotal role in the entire process, as catalase selectively breaks down the hydrogen peroxide generated during electrolysis into water and oxygen.[19].

4. Conclusions

This study has focused on enhancing the eradication of bacterial biofilms through innovative approaches involving polymer coatings on the anode. The first approach is centered on the electrochemical generation of reactive oxygen species (ROS) at the anode's surface. This method involves a metallized polytetrathienylporphyrin layer with ROS generation capabilities. The investigation revealed that poly-3TTP/Fe, among the metallized polytetrathienylporphyrin layers, demonstrates the highest propensity to catalyze the formation of H_2O_2, a crucial component in biofilm eradication. Importance of electrogenerated H_2O_2 in biofilm destruction was demonstrated by the addition of catalase, which attenuated biocidal effect of DC. The second approach, termed cation generation, employs an insoluble and hydrophobic ferrocene polyamide (Fc-PA) coating derived from 1,6-diaminohexane and 1,1′-ferrocenedicarboxylic acid. This hydrophobic structure transforms into a bactericidal, hydrolytically degradable polycation upon oxidation. Remarkably, the catalytically active poly-3TTP/Fe film retains its integrity, while the ferrocene polyamide coating exhibits visible ablation, which is consistent with the proposed mechanism of action. Both of these approaches show promising potential in enhancing the electro-mediated eradication of *Staphylococcus aureus* biofilms. By catalyzing ROS generation and utilizing innovative cation generation techniques, this research contributes to addressing the challenge of biofilm-associated infections, particularly in the context of medical implants.

CRediT authorship contribution statement

Stephane Hoang: Methodology, Investigation, Data curation. **Hanna Zhukouskaya:** Methodology, Investigation, Data curation. **Iryna Ivanko:** Writing – original draft, Methodology, Investigation, Data curation. **Jan Svoboda:** Writing – original draft, Methodology, Investigation, Data curation. **Michaela Hympánová:** Methodology, Investigation, Data curation. **Jan Marek:** Writing – original draft, Methodology, Investigation, Data curation. **Ondřej Soukup:** Writing – review & editing, Writing – original draft, Formal analysis, Data curation. **Miroslav Šlouf:** Methodology, Investigation, Data curation. **Jan Kotek:** Writing – original draft, Methodology, Investigation, Data curation. **Eric Doris:** Writing – review & editing, Conceptualization. **Edmond Gravel:** Writing – review & editing, Conceptualization. **Elena Tomšík:** Writing – review & editing, Writing – original draft, Funding acquisition, Conceptualization. **Martin Hrubý:** Writing – review & editing, Writing – original draft, Funding acquisition, Conceptualization.

Declaration of competing interest

The authors declare that they have no known competing financial interests or personal relationships that could have appeared to influence the work reported in this paper.

Data availability

Data will be made available on request.

Acknowledgements

M.H. and J.K. thank Czech Science Foundation (GAČR, 21–01090S) for financial support . M.H. thanks for financial support the Ministry of Education, Youth and Sports of the Czech Republic (MEYS, LUAUS24272). M.H., E.T. and H.Z thank the project New Technologies for Translational Research in Pharmaceutical Sciences/NETPHARM, project ID CZ.02.01.01/00/22_008/0004607, co-funded by the European Union, for financial support. J.M., O.S. and M.Hy. acknowledge to the Ministry of Defence of the Czech Republic "Long Term Organization Development Plan 1011" – Healthcare Challenges of WMD II of the Military Faculty of Medicine Hradec Kralove, University of Defence, Czech Republic (Project No: DZRO-FVZ22-ZHN II), and MH CZ – DRO (UHHK, 00179906).

Appendix A. Supplementary material

Supplementary data to this article can be found online at https://doi.org/10.1016/j.eurpolymj.2024.112910.

References

[1] A.D. Verderosa, M. Totsika, K.E. Fairfull-Smith, Bacterial biofilm eradication agents: A current review, Front. Chem. 7 (2019) 824, https://doi.org/10.3389/fchem.2019.00824.
[2] A.A. Ciarolla, N. Lapin, D. Williams, R. Chopra, D.E. Greenberg, Physical approaches to prevent and treat bacterial biofilm, Antibiotics-Basel 12 (1) (2023) 54, https://doi.org/10.3390/antibiotics12010054.
[3] L. Yang, Y. Liu, H. Wu, Z.J. Song, N. Hoiby, S. Molin, M. Givskov, Combating biofilms, FEMS Immunol. Med. Microbiol. 65 (2) (2012) 146–157, https://doi.org/10.1111/j.1574-695X.2011.00858.x.
[4] B.P. Conlon, S.E. Rowe, K. Lewis, Persister Cells in Biofilm Associated Infections, in: G. Donelli (Ed.), Biofilm-Based Healthcare-Associated Infections, Vol Ii, Springer-Verlag Berlin, Berlin, 2015, pp. 1-9. https://doi.org/10.1007/978-3-319-09782-4_1.
[5] R. Srinivasan, S. Santhakumari, P. Poonguzhali, M. Geetha, M. Dyavaiah, X.M. Lin, Bacterial biofilm inhibition: a focused review on recent therapeutic strategies for combating the biofilm mediated infections, Front. Microbiol. 12 (2021) 676458, https://doi.org/10.3389/fmicb.2021.676458.
[6] S. Veerachamy, T. Yarlagadda, G. Manivasagam, P. Yarlagadda, Bacterial adherence and biofilm formation on medical implants: a review, Proc. Inst. Mech. Eng. Part H-J. Eng. Med. 228 (10) (2014) 1083–1099, https://doi.org/10.1177/0954411914556137.
[7] S. Bernardi, E. Qorri, G. Botticelli, A. Scarano, G. Marzo, R. Gatto, A.G. Lucchina, C. Mortellaro, E. Lupi, C. Rastelli, G. Falisi, Use of electrical field for biofilm implant removal, Eur. Rev. Med. Pharmacol. Sci. 27 (2023) 114–121, https://doi.org/10.26355/eurrev_202304_31328.
[8] J.S. Dhaliwal, N.A. Abd Rahman, L.C. Ming, S.K.S. Dhaliwal, J. Knights, R.F. A. Junior, Microbial biofilm decontamination on dental implant surfaces: A mini review, Front. Cell. Infect. Microbiol. 11 (2021) 736186, https://doi.org/10.3389/fcimb.2021.736186.
[9] D. Freebairn, D. Linton, E. Harkin-Jones, D.S. Jones, B.F. Gilmore, S.P. Gorman, Electrical methods of controlling bacterial adhesion and biofilm on device surfaces, Expert Rev. Med. Devices 10 (1) (2013) 85–103, https://doi.org/10.1586/erd.12.70.
[10] S. Sinha, R. Kumar, J. Anand, R. Gupta, A. Gupta, K. Pant, S. Dohare, P. Tiwari, K. K. Kesari, S. Krishnan, P.K. Gupta, Nanotechnology-based solutions for antibiofouling applications: An overview, ACS Appl. Nano Mater. 6 (14) (2023) 12828–12848, https://doi.org/10.1021/acsanm.3c01539.
[11] A. Banerjee, P. Chowdhury, K. Bauri, B. Saha, P. De, Inhibition and eradication of bacterial biofilm using polymeric materials, Biomater. Sci. 11 (1) (2022) 11–36, https://doi.org/10.1039/d2bm01276f.
[12] S. Watts, M. Gontsarik, A. Lassenberger, J.D.P. Valentin, A. Wolfensberger, S. D. Brugger, M. Zabara, W. Pronk, S. Salentinig, Scalable synthesis of self-disinfecting polycationic coatings for hospital relevant surfaces, Adv. Mater. Interfaces 10 (8) (2023) 2202299, https://doi.org/10.1002/admi.202202299.
[13] V. Choi, J.L. Rohn, P. Stoodley, D. Carugo, E. Stride, Drug delivery strategies for antibiofilm therapy, Nat. Rev. Microbiol. 21 (9) (2023) 555–572, https://doi.org/10.1038/s41579-023-00905-2.
[14] A. Upadhyay, D. Pal, A. Kumar, Combinatorial enzyme therapy: A promising neoteric approach for bacterial biofilm disruption, Process Biochem. 129 (2023) 56–66, https://doi.org/10.1016/j.procbio.2023.02.022.
[15] J. Swartjes, T. Das, S. Sharifi, G. Subbiahdoss, P.K. Sharma, B.P. Krom, H. J. Busscher, H.C. van der Mei, A functional DNase I coating to prevent adhesion of bacteria and the formation of biofilm, Adv. Funct. Mater. 23 (22) (2013) 2843–2849, https://doi.org/10.1002/adfm.201202927.
[16] B. van Dijk, J.V.C. Lemans, R.M. Hoogendoorn, E. Dadachova, J.M.H. de Klerk, H. C. Vogely, H. Weinans, M. Lam, B.C.H. van der Wal, Treating infections with ionizing radiation: a historical perspective and emerging techniques, Antimicrob. Resist. Infect. Control 9 (1) (2020) 121, https://doi.org/10.1186/s13756-020-00775-w.
[17] S.G. Joshi, M. Paff, G. Friedman, G. Fridman, A. Fridman, A.D. Brooks, Control of methicillin-resistant Staphylococcus aureus in planktonic form and biofilms: A biocidal efficacy study of nonthermal dielectric-barrier discharge plasma, Am. J. Infect. Control 38 (4) (2010) 293–301, https://doi.org/10.1016/j.ajic.2009.11.002.
[18] J.L. Del Pozo, M.S. Rouse, R. Patel, Bioelectric effect and bacterial biofilms. A systematic review, Int. J. Artif. Organs 31 (9) (2008) 786–795, https://doi.org/10.1177/039139880803100906.

[19] C.L. Brinkman, S.M. Schmidt-Malan, M.J. Karau, K. Greenwood-Quaintance, D. J. Hassett, J.N. Mandrekar, R. Patel, Exposure of bacterial biofilms to electrical current leads to cell death mediated in part by reactive oxygen species, PLoS One 11 (12) (2016) e0168595.
[20] J. Jass, J.W. Costerton, H.M. Lappinscott, The effect of electrical currents and tobramycin on Pseudomonas-aeruginosa biofilms, J. Indust. Microbiol. 15 (3) (1995) 234–242, https://doi.org/10.1007/bf01569830.
[21] T. Urbanek, I. Ivanko, J. Svoboda, E. Tomsik, M. Hruby, Selective potentiometric detection of reactive oxygen species (ROS) in biologically relevant concentrations by a modified metalized polyporphyrine sensing layer coated with nonbiofouling poly (2-alkyl-2oxazoline)s, Sens. Actuator B-Chem. 363 (2022) 131827, https://doi.org/10.1016/j.snb.2022.131827.
[22] P.D. Josephy, T. Eling, R.P. Mason, The horseradish peroxidase-catalyzed oxidation of 3,5,3',5'-tatramethylbenzidine – free-radical and charge-transfer intermediates, J. Biol. Chem. 257 (7) (1982) 3669–3675, https://doi.org/10.1016/S0021-9258(18)34832-4.
[23] P. Svec, O.V. Petrov, J. Lang, P. Stepnicka, O. Groborz, D. Dunlop, J. Blahut, K. Kolouchova, L. Loukotova, O. Sedlacek, T. Heizer, Z. Tosner, M. Slouf, H. Benes, R. Hoogenboom, M. Hruby, Fluorinated ferrocene moieties as a platform for redox-responsive polymer F-19 MRI theranostics, Macromolecules 55 (2) (2022) 658–671, https://doi.org/10.1021/acs.macromol.1c01723.
[24] K. Kolouchova, O. Groborz, Z. Cernochova, A. Skarkova, J. Brabek, D. Rosel, P. Svec, Z. Starcuk, M. Slouf, M. Hruby, Thermo- and ROS-responsive self-assembled polymer nanoparticle tracers for F-19 MRI theranostics, Biomacromolecules 22 (6) (2021) 2325–2337, https://doi.org/10.1021/acs.biomac.0c01316.